

# Bootstrapped Newtonian stars and black holes

Roberto Casadio<sup>ab\*</sup>, Michele Lenzi<sup>ab†</sup> and Octavian Micu<sup>c‡</sup>

<sup>a</sup>*Dipartimento di Fisica e Astronomia, Università di Bologna  
via Irnerio 46, 40126 Bologna, Italy*

<sup>b</sup>*I.N.F.N., Sezione di Bologna, I.S. FLAG  
viale B. Pichat 6/2, 40127 Bologna, Italy*

<sup>c</sup>*Institute of Space Science, Bucharest, Romania  
P.O. Box MG-23, RO-077125 Bucharest-Magurele, Romania*

December 15, 2024

## Abstract

We study equilibrium configurations of a homogenous ball of matter in a bootstrapped description of gravity which includes a gravitational self-interaction term beyond the Newtonian coupling. Both matter density and pressure are accounted for as sources of the gravitational potential for test particles. Unlike the general relativistic case, no Buchdahl limit is found and the pressure can in principle support a star of arbitrarily large compactness. By defining the horizon as the location where the escape velocity of test particles equals the speed of light, like in Newtonian gravity, we find a minimum value of the compactness for which this occurs. The solutions for the gravitational potential here found could effectively describe the interior of macroscopic black holes in the quantum theory, as well as predict consequent deviations from general relativity in the strong field regime of very compact objects.

*PACS - 04.70.Dy, 04.70.-s, 04.60.-m*

## 1 Introduction and motivation

The true nature of black holes is already problematic in the classical description given by general relativity and notoriously more so once one tries to incorporate the unavoidable quantum physics. Once a trapping surface appears, singularity theorems of general relativity require an object to collapse all the way into a region of vanishing volume and infinite density [1]. At the same time, a point-like source is well known to be classically unacceptable [2]. One would therefore hope that quantum physics cures this problem, the same way it makes the hydrogen atom stable, by affecting the gravitational dynamics, at least in the strong field regime (where the description of matter likely requires physics beyond the standard model as well [3]).

---

\*E-mail: casadio@bo.infn.it

†E-mail: michele.lenzi@studio.unibo.it

‡E-mail: octavian.micu@spacescience.ro

In light of the above observations, in Ref. [4] we studied an effective equation for the gravitational potential of a static source which contains a gravitational self-interaction term besides the usual Newtonian coupling with the matter density. Following an idea from Ref. [5], this equation was derived in details from a Fierz-Pauli Lagrangian in Ref. [6], and it can therefore be viewed as stemming from the truncation of the relativistic theory at some “post-Newtonian” order (for the standard post-Newtonian formalism, see Ref. [7]). However, since the “post-Newtonian” correction  $V_{\text{PN}} \sim M^2/r^2$  is positive and grows faster than the Newtonian potential  $V_{\text{N}} \sim M/r$  near the surface of the source, one is allowed to consider only matter sources with radius  $R \gg R_{\text{H}}$  in this approximation (where we remark that  $M$  is the total ADM mass [8] of the system and

$$R_{\text{H}} \equiv 2 G_{\text{N}} M \quad (1.1)$$

is the gravitational radius of the source.) This consistency condition clearly excludes the possibility to study very compact matter sources and, in particular, those with  $R \simeq R_{\text{H}}$  which are on the verge of forming a black hole. For the ultimate purpose of including such cases and gain some hindsight about the fate of matter which collapses inside a black hole, in Ref. [4] we studied the non-linear equation of the effective theory derived in Ref. [6] at face value, without requiring that the corrections it introduces with respect to the Newtonian potential remain small.

In Ref. [4], we showed that the qualitative behaviour of the complete solutions to that non-linear equation resembles rather closely the Newtonian counterpart. This result, which essentially stems from including a gravitational self-interaction in the Poisson equation, is what we call “bootstrapping” the Newtonian gravity, which could be viewed as the first step in the perturbative reconstruction of general relativity (see *e.g.*, Refs. [9]). However, it could also be conjectured that it effectively describes the (mean field) quantum gravitational potential of such extremely compact objects after the break-down of classical general relativity. Moreover, we found no equivalent of the Buchdahl limit [10] of general relativity, and this result implies that matter pressure (possibly of quantum origin) could support sources of arbitrarily large compactness  $G_{\text{N}} M/R \gg 1$ .

Another (rather expected) result found in Ref. [4] is that the pressure becomes the dominant source of energy when  $R \lesssim R_{\text{H}}$ . For this reason, we here modify the effective theory in order to consistently supplement the matter density with the pressure as sources of the gravitational potential. We then study systems with generic compactness  $G_{\text{N}} M/R$ , from the regime  $R \gg R_{\text{H}}$ , in which we recover the standard post-Newtonian picture, to  $R \ll R_{\text{H}}$  where we find the source is enclosed within a horizon. The latter is defined according to the Newtonian view as the location at which the escape velocity of test particles equals the speed of light. Of course, it should be possible to treat the single microscopic constituents of the source in this test particle approximation and the presence of an horizon therefore refers to their inability to escape the gravitational pull.

Like in Refs. [4, 6], we shall just consider (static) spherically symmetric systems, so that all quantities depend only on the radial coordinate  $r$ , and the matter density  $\rho = \rho(r)$  will also be assumed homogenous inside the source ( $r \leq R$ ) for the sake of simplicity. The pressure will instead be determined consistently from the condition of staticity. The paper is organised as follows: in Section 2, we briefly review the derivation of the equation for the potential with the inclusion of a pressure term; in Section 3, we solve for the outer and inner potential generated by the homogenous source using appropriate analytical methods for the diverse regimes. In particular, we study intermediate and large compact sources with  $R \lesssim R_{\text{H}}$  as possible candidates for effectively describing collapsed objects which should act as black holes according to general relativity; their horizon structure is then analysed in Section 4; we finally comment about our results and possible outlooks in Section 5.

## 2 Bootstrapped theory for the gravitational potential

From Ref. [6], we recall that the non-linear equation for the potential  $V = V(r)$  describing the gravitational pull on test particles generated by a matter density  $\rho = \rho(r)$  can be obtained starting from the Newtonian Lagrangian

$$L_N[V] = -4\pi \int_0^\infty r^2 dr \left[ \frac{(V')^2}{8\pi G_N} + \rho V \right], \quad (2.1)$$

where  $f' \equiv df/dr$ , and the corresponding equation of motion is the Poisson equation

$$r^{-2} (r^2 V')' \equiv \Delta V = 4\pi G_N \rho \quad (2.2)$$

for the Newtonian potential  $V = V_N$ . We can then include the effects of gravitational self-interaction by noting that the Hamiltonian

$$H_N[V] = -L_N[V] = 4\pi \int_0^\infty r^2 dr \left( -\frac{V \Delta V}{8\pi G_N} + \rho V \right), \quad (2.3)$$

computed on-shell by means of Eq. (2.2), yields the Newtonian potential energy

$$\begin{aligned} U_N(r) &= 2\pi \int_0^r \bar{r}^2 d\bar{r} \rho(\bar{r}) V(\bar{r}) \\ &= -\frac{1}{2G_N} \int_0^r \bar{r}^2 d\bar{r} [V'(\bar{r})]^2, \end{aligned} \quad (2.4)$$

where we used Eq. (2.2) and then integrated by parts discarding boundary terms. One can view the above  $U_N$  as given by the interaction of the matter distribution enclosed in a sphere of radius  $r$  with the gravitational field. Following Ref. [5] (see also Ref. [11]), we then define a self-gravitational source proportional to the gravitational energy  $U_N$  per unit volume, that is

$$J_V \simeq \frac{dU_N}{dV} = -\frac{[V'(r)]^2}{2\pi G_N}. \quad (2.5)$$

In Ref. [4], we found that the pressure  $p$  becomes very large for compact sources with a size  $R \lesssim R_H$ , where  $R_H$  is the gravitational radius of Eq. (1.1), and we must therefore add a corresponding potential energy  $U_B$  such that

$$p = -\frac{dU_B}{dV}. \quad (2.6)$$

Since the latter contribution just adds to  $\rho$ , it can be easily included by simply shifting  $\rho \rightarrow \rho + p$ . Upon including these new source terms, and the analogous higher order term  $J_\rho = -2V^2$  which couples with the matter source, we obtain the total Lagrangian [6]

$$\begin{aligned} L[V] &= L_N[V] - 4\pi \int_0^\infty r^2 dr [q_\Phi J_V V + q_\Phi J_\rho (\rho + p)] \\ &= -4\pi \int_0^\infty r^2 dr \left[ \frac{(V')^2}{8\pi G_N} (1 - 4q_\Phi V) + (\rho + p) V (1 - 2q_\Phi V) \right], \end{aligned} \quad (2.7)$$

where the parameter  $q_\Phi$  plays the role of a coupling constant <sup>1</sup> for the graviton current  $J_V$  and the higher-order matter current  $J_\rho$ . The associated effective hamiltonian is simply given by

$$H[V] = -L[V] \quad (2.8)$$

Finally, the Euler-Lagrange equation for  $V$  is given by

$$\Delta V = 4\pi G_N (\rho + p) + \frac{2q_\Phi (V')^2}{1 - 4q_\Phi V} \quad (2.9)$$

and the conservation equation that determines the pressure reads

$$p' = -V'(\rho + p) . \quad (2.10)$$

Although we showed the parameter  $q_\Phi$  for clarity, we shall only consider the case  $q_\Phi = 1$  in the following.

### 3 Homogeneous ball in vacuum

Since we are interested in compact sources, we will consider the simplest case in which the matter density is homogeneous and vanishes outside the sphere of radius  $r = R$ , that is

$$\rho = \rho_0 \equiv \frac{3M_0}{4\pi R^3} \Theta(R - r) , \quad (3.1)$$

where  $\Theta$  is the Heaviside step function, and

$$M_0 = 4\pi \int_0^R r^2 dr \rho(r) . \quad (3.2)$$

The relevant solutions must also satisfy the regularity condition in the centre

$$V'_{\text{in}}(0) = 0 \quad (3.3)$$

and be smooth across the surface  $r = R$ , that is

$$V_{\text{in}}(R) = V_{\text{out}}(R) \equiv V_R \quad (3.4)$$

$$V'_{\text{in}}(R) = V'_{\text{out}}(R) \equiv V'_R , \quad (3.5)$$

where we defined  $V_{\text{in}} = V(0 \leq r \leq R)$  and  $V_{\text{out}} = V(R \leq r)$ .

---

<sup>1</sup>Different values of  $q_\phi$  can be implemented in order to obtain the approximate potential for different motions of the test particles in general relativity.

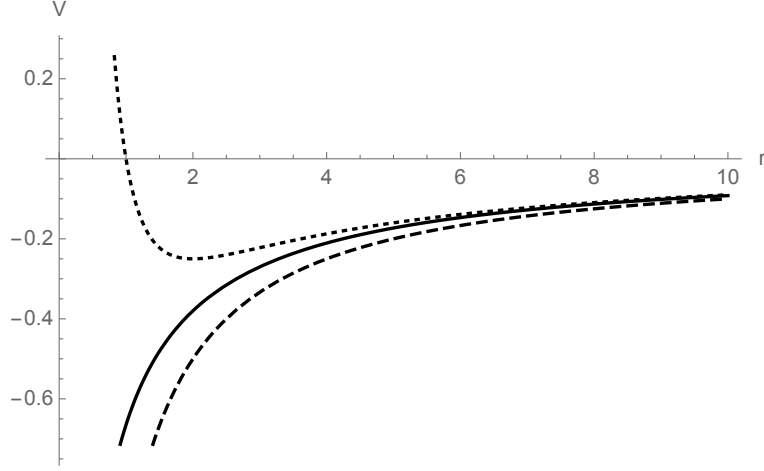


Figure 1: Potential  $V_{\text{out}}$  (solid line) *vs* Newtonian potential (dashed line) *vs* order  $G_N^2$  expansion of  $V_{\text{out}}$  (dotted line) for  $r > 0$  (all quantities are in units of  $G_N M$ ).

### 3.1 Outer vacuum solution

In the vacuum, where  $\rho = p = 0$ , Eq. (2.10) is trivially satisfied and Eq. (2.9) with  $q_\Phi = 1$  reads

$$\Delta V = \frac{2(V')^2}{1 - 4V}, \quad (3.6)$$

which is exactly solved by

$$V_{\text{out}} = \frac{1}{4} \left[ 1 - \left( 1 + \frac{6 G_N M}{r} \right)^{2/3} \right]. \quad (3.7)$$

where two integration constants were fixed by requiring the expected Newtonian behaviour in terms of the ADM-like mass  $M$  for large  $r$ . In fact, the large  $r$  expansion now reads

$$V_{\text{out}} \underset{r \rightarrow \infty}{\simeq} -\frac{G_N M}{r} + \frac{G_N^2 M^2}{r^2} - \frac{8 G_N^3 M^3}{3 r^3}, \quad (3.8)$$

and contains the expected post-Newtonian term  $V_{\text{PN}}$  of order  $G_N^2$  without any further assumptions [6].

From Eq. (3.7), we also obtain

$$V_R = V_{\text{out}}(R) = \frac{1}{4} \left[ 1 - \left( 1 + \frac{6 G_N M}{R} \right)^{2/3} \right], \quad (3.9)$$

and

$$V'_R = V'_{\text{out}}(R) = \frac{G_N M}{R^2 (1 + 6 G_N M/R)^{1/3}}, \quad (3.10)$$

which we will often use since they appear in the boundary conditions (3.4) and (3.5).

### 3.2 The inner pressure

We first consider the conservation Eq. (2.10) and notice that, for  $0 \leq r \leq R$ , we can write it as

$$\frac{(\rho_0 + p)'}{\rho_0 + p} = -V' , \quad (3.11)$$

which allows us to express the total effective energy density as

$$\rho_0 + p = \alpha e^{-V} . \quad (3.12)$$

The integration constant can be determined by imposing the usual boundary condition

$$p(R) = 0 , \quad (3.13)$$

which finally yields

$$p = \rho_0 [e^{V_R - V} - 1] , \quad (3.14)$$

where  $V_R$  is given in Eq. (3.9).

### 3.3 The inner potential

The field equation (2.9) for  $0 \leq r \leq R$  and  $q_\Phi = 1$  becomes

$$\begin{aligned} \Delta V &= 4\pi G_N \rho_0 e^{V_R - V} + \frac{2(V')^2}{1 - 4V} \\ &= \frac{3G_N M_0}{R^3} e^{V_R - V} + \frac{2(V')^2}{1 - 4V} , \end{aligned} \quad (3.15)$$

and we notice that  $\rho_0 e^{V_R} < \rho_0$  since  $V_R < 0$ . The relevant solutions  $V_{\text{in}}$  to Eq. (3.15) must also satisfy the regularity condition (3.3) and the matching conditions (3.4) and (3.5), with  $V_R$  and  $V'_R$  respectively given in Eq. (3.9) and (3.10). Since Eq. (3.15) is a second order (ordinary) differential equation, the three boundary conditions (3.3), (3.4) and (3.5) will not only fix the potential  $V_{\text{in}}$  uniquely, but also the ratio of the proper mass parameter  $G_N M_0/R$  for any given value of the compactness  $G_N M/R$ .

It is hard to find the complete solution of the above problem for general compactness. An approximate analytic solution to Eq. (3.15) can be found quite straightforwardly only in the regimes of low and intermediate compactness (*i.e.* for  $G_N M/R \ll 1$  and  $G_N M/R \simeq 1$ ). On the other hand, for  $G_N M \gg R$ , the non-linearity of Eq. (3.15) and the interplay between  $M_0$  and the boundary conditions (3.3), (3.4) and (3.5) make it very difficult to find any (approximate or numerical) solutions. In fact, even a slight error in the estimate of  $M_0 = M_0(M, R)$  can spoil the solution completely. For this reason, we will take advantage of the comparison method [12–14] which essentially consists in finding two bounding functions  $V_\pm$  (upper and lower approximate solutions), such that  $E_+(r) < 0$  and  $E_-(r) > 0$  for  $0 \leq r \leq R$ , where

$$E_\pm \equiv \Delta V_\pm - \frac{3G_N M_0^\pm(M)}{R^3} e^{V_R - V_\pm} - \frac{2(V'_\pm)^2}{1 - 4V_\pm} . \quad (3.16)$$

Comparison theorems then guarantee that the proper solution will lie in between the two bounding functions (see Appendix B for more details), that is

$$V_- < V_{\text{in}} < V_+ . \quad (3.17)$$

The advantage of this method is twofold. It will serve as a tool for finding approximate solutions in the regime of large compactness and will also allow us to check the accuracy of the approximate analytic solution for low and intermediate compactness.

### 3.3.1 Small and intermediate compactness

For the radius  $R$  of the source much larger or of the order of  $G_{\text{N}} M$ , an analytic approximation  $V_{\text{s}}$  for the solution  $V_{\text{in}}$  can be found by simply expanding around  $r = 0$ , and turns out to be

$$V_{\text{s}} = V_0 + \frac{G_{\text{N}} M_0}{2 R^3} e^{V_R - V_0} r^2 . \quad (3.18)$$

where  $V_0 \equiv V_{\text{in}}(0) < 0$  and  $V_R$  is given in Eq. (3.9). We remark that the regularity condition (3.3) requires that all terms of odd order in  $r$  in the Taylor expansion about  $r = 0$  must vanish.

We can immediately notice that the above form is qualitatively similar to the Newtonian solution recalled in Appendix A. Like the latter, the present case does not show any singularity in the potential for  $r = 0$  and the pressure,

$$p \simeq \rho_0 \left[ e^{V_R - V_0 - B r^2} - 1 \right] , \quad (3.19)$$

is also regular in  $r = 0$ ,

$$p(0) = \rho_0 \left[ e^{-(V_0 - V_R)} - 1 \right] > 0 , \quad (3.20)$$

since  $V_0 < V_R < 0$ .

The two matching conditions at  $r = R$  can now be written as

$$\begin{cases} 2 R (V_R - V_0) \simeq G_{\text{N}} M_0 e^{V_R - V_0} \\ R^2 V'_R \simeq G_{\text{N}} M_0 e^{V_R - V_0} , \end{cases} \quad (3.21)$$

One can solve the second equation of the system above for  $V_0$  to obtain

$$V_0 = \frac{1}{4} \left[ 1 - (1 + 6 G_{\text{N}} M/R)^{2/3} \right] + \ln \left[ \frac{M_0}{M} (1 + 6 G_{\text{N}} M/R)^{1/3} \right] , \quad (3.22)$$

which is written in terms of  $M_0$  and  $M$ . Using the first equation in (3.21), one then finds

$$M_0 = \frac{M e^{-\frac{G_{\text{N}} M}{2 R (1 + 6 G_{\text{N}} M/R)^{1/3}}}}{(1 + 6 G_{\text{N}} M/R)^{1/3}} . \quad (3.23)$$

This last expression, along with the one for  $V_0$ , can be used to write the approximate solution (3.18) in terms of  $M$  only as

$$V_{\text{s}} = \frac{R^3 \left[ (1 + 6 G_{\text{N}} M/R)^{1/3} - 1 \right] + 2 G_{\text{N}} M (r^2 - 4 R^2)}{4 R^3 (1 + 6 G_{\text{N}} M/R)^{1/3}} , \quad (3.24)$$

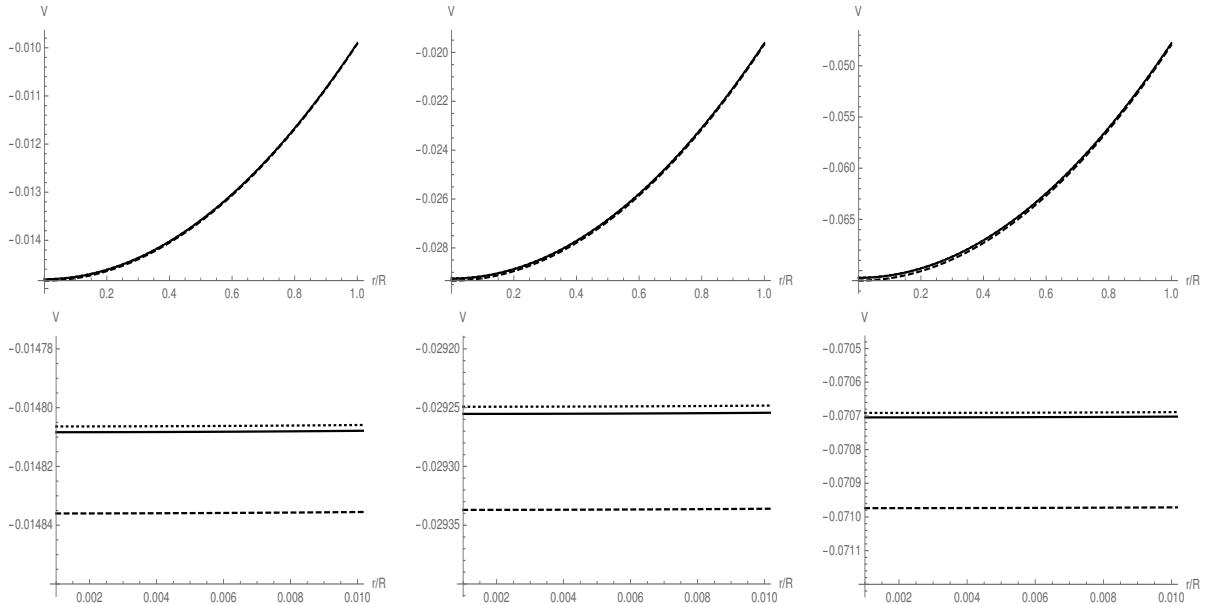


Figure 2: Numerical solution to Eq. (3.15) (solid line) *vs* approximate solution  $V_s = V_+$  in Eq. (3.24) (dotted line) *vs* lower bounding function  $V_- = C V_s$  (dashed line), for  $G_N M/R = 1/100$  (top left panel, with  $C = 1.002$ ),  $G_N M/R = 1/50$  (top central panel, with  $C = 1.003$ ) and  $G_N M/R = 1/20$  (top right panel, with  $C = 1.004$ ). The bottom panels show the region  $0 \leq r \leq R/100$  where the difference between the three potentials is the largest.

where we remark that this expression contains only the terms of the first two orders in the series expansion about  $r = 0$ .

We can now estimate the accuracy of the approximation (3.18) by means of the comparison method. The plots in Fig. 2 and 3 show that  $V_s$  is already in good agreement with the numerical solution for both small and intermediate compactness and the smaller the ratio  $G_N M/R$ , the less  $V_s$  differs from the numerical solution. Indeed, the approximate solution  $V_s$  fails in the large compactness regime, which will be studied in the next subsection. The same plots also tell us that  $V_s$  is actually an upper bounding function  $V_+$  up to  $G_N M/R \simeq 1/20$ , but becomes a lower bounding function  $V_-$  for higher compactness (this can be verified by showing that it satisfies the required conditions described in Appendix B). The other bounding function ( $V_-$  or  $V_+$ ) can be found by simply multiplying  $V_s$  by a suitable constant factor  $C$  determined according to the theorem in Appendix B (with  $C > 1$  for small compactness and  $C < 1$  for intermediate compactness). This means that the approximate solution (3.18) overestimates the expected true potential  $V_{\text{in}}$  for low compactness, whereas it underestimates  $V_{\text{in}}$  when the compactness grows beyond  $G_N M/R \simeq 1/20$ . We also note that the gap between the above  $V_-$  and  $V_+$  increases for increasing compactness, which signals the need for a better estimate of  $M_0 = M_0(M)$  in order to narrow this gap and gain more precision for describing the intermediate compactness. The latter regime is particularly useful for understanding objects that have collapsed to a size of the order of their gravitational radius<sup>2</sup>. We should remark that, in this analysis, we actually employed the comparison method in the whole

<sup>2</sup>The uniform density profile (3.1) can also be viewed as a crude approximation of the density in the corpuscular model of black holes, in which the energy is distributed throughout the entire inner volume [15–23].



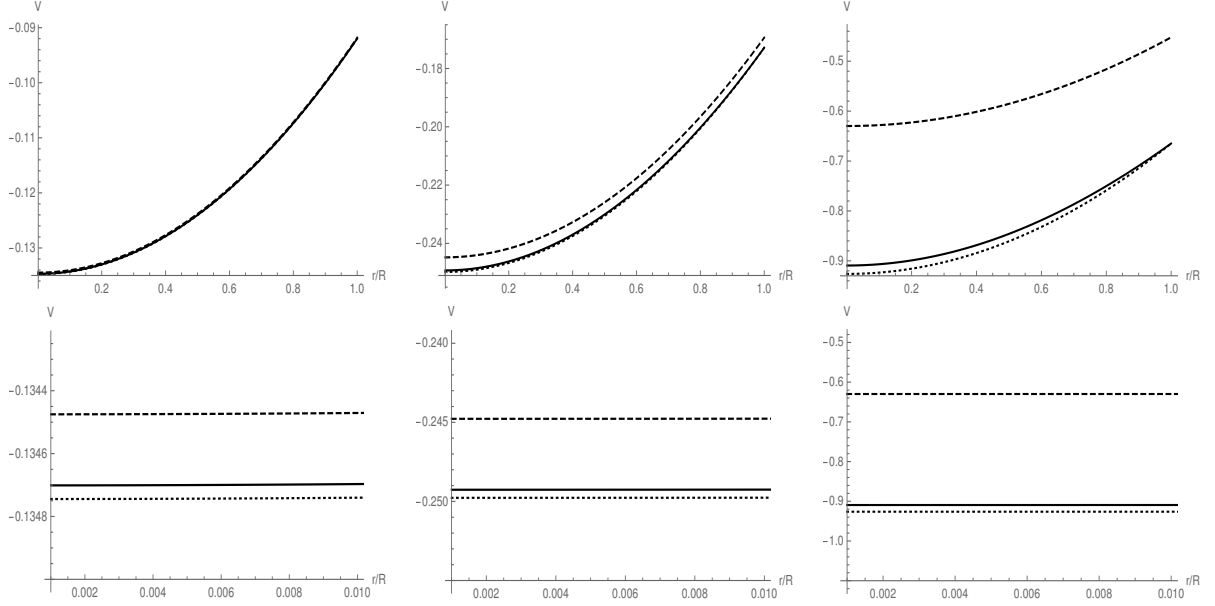


Figure 3: Numerical solution to Eq. (3.15) (solid line) *vs* approximate solution  $V_s = V_-$  in Eq. (3.24) (dotted line) *vs* upper bounding function  $V_+ = C V_s$  (dashed line), for  $G_N M/R = 1/10$  (top left panel, with  $C = 0.998$ ),  $G_N M/R = 1/5$  (top central panel, with  $C = 0.980$ ) and  $G_N M/R = 1$  (top right panel, with  $C = 0.680$ ). The bottom panels show the region  $0 < r < R/100$  where the difference between the three expressions is the largest.

range  $0 \leq r < \infty$  by defining  $V_{\pm} = C_{\pm} V_{\text{out}}$ , for  $r > R$ , where  $V_{\text{out}}$  is the exact solution in Eq. (3.7) (see Fig. 4). This means that we did not require that the lower function  $V_-$  (for  $G_N M/R \lesssim 1/20$ ) and the upper function  $V_+$  (for  $G_N M/R \gtrsim 1/20$ ) satisfy the boundary conditions (3.4) and (3.5) at  $r = R$ . However, since we have the analytical form for  $V_{\text{out}}$  in its entire range of applicability, all that is needed to ensure that  $V_{\pm}$  are the upper and lower bounding functions is for the constants  $C_{\pm}$  which multiply the expression for  $V_{\text{out}}$  to be smaller, respectively larger than one.

As stated earlier, the analytic approximation (3.24) works best in the regime of small compactness, in which we can further Taylor expand all quantities to second order in  $G_N M/R \ll 1$  to obtain

$$V_0 \simeq -\frac{3 G_N M}{2 R} \left( 1 - \frac{4 G_N M}{3 R} \right), \quad (3.25)$$

and finally use Eq. (3.23) to obtain

$$M_0 \simeq M \left( 1 - \frac{5 G_N M}{2 R} \right), \quad (3.26)$$

in qualitative agreement with the result of Ref. [4], where however the effect of the pressure on the potential was neglected.

The above expressions for  $M_0$  and  $V_0$  can be used to write the inner potential (3.18) in a much simpler form in terms of  $M$  as

$$V_{\text{in}} \simeq -\frac{3 G_N M}{2 R} + \frac{2 G_N^2 M^2}{R^2} + \frac{G_N M (R - 2 G_N M)}{2 R^4} r^2. \quad (3.27)$$

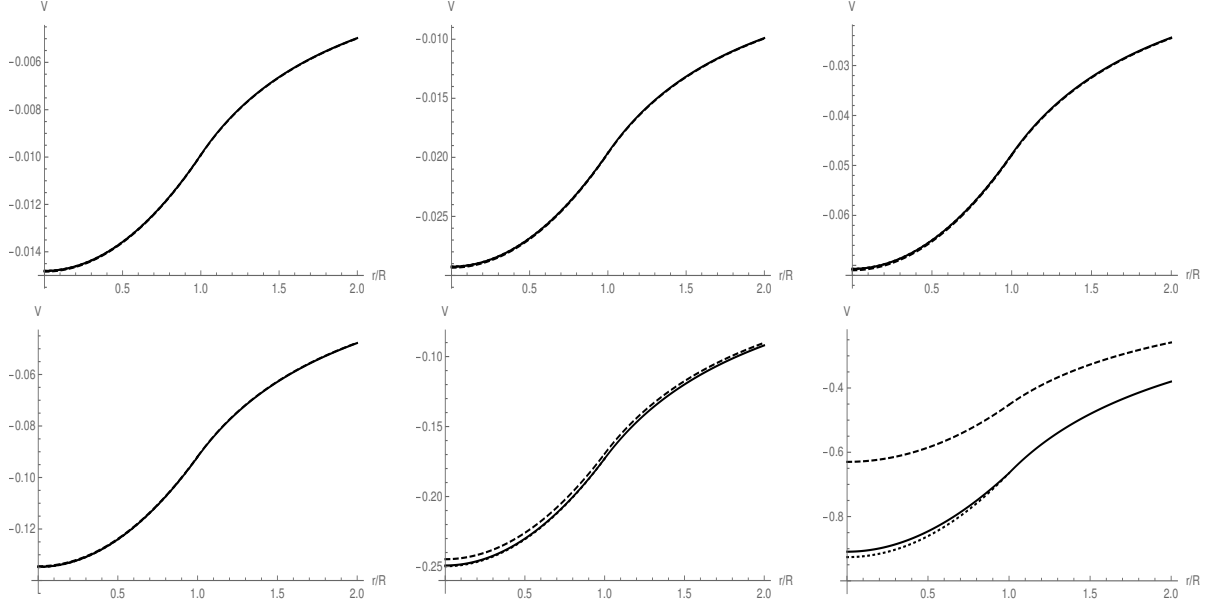


Figure 4: Numerical solution to Eq. (3.15) (solid line) *vs* approximate solution  $V_s$  in Eq. (3.24) (dotted line) *vs* other bounding function  $V_{\pm}$  (dashed line), for  $G_N M/R = 1/100$  (top left panel),  $G_N M/R = 1/50$  (top central panel),  $G_N M/R = 1/20$  (top right panel),  $G_N M/R = 1/10$  (bottom left panel),  $G_N M/R = 1/5$  (bottom central panel) and  $G_N M/R = 1$  (bottom right panel).

As expected, the solution for small compactness, which can be useful for describing stars with a radius orders of magnitude larger in size than their gravitational radius, qualitatively tracks the Newtonian case. This can also be seen from Fig. 5. The limitations of the small compactness approximation can be inferred from Eq. (3.27). For  $2 G_N M \equiv R_H \sim R$  the last term vanishes and  $V_{\text{in}}$  becomes a constant.

Finally, it is important to remark that, as opposed to what was done in Ref. [4], the pressure now acts as a source and can be consistently evaluated with the help of Eqs. (3.14) and (3.18). The plots in Fig. 6 clearly show that the pressure can be well approximated by the Newtonian formula in the regime of low compactness, to wit

$$p \simeq \frac{3 G_N M^2 (R^2 - r^2)}{8 \pi R^6}, \quad (3.28)$$

again in qualitative agreement with Ref. [4]. Nevertheless, the same plots indicate that it rapidly departs from the Newtonian expression when we approach the regime of intermediate compactness, while remaining almost identical to the numerical approximation.

### 3.3.2 Large compactness

For  $G_N M/R \gg 1$ , rather than employing a Taylor expansion like we did for small compactness, it is more convenient to fully rely on comparison methods [12–14] and start from the exact solution of the simpler equation

$$\psi'' = \frac{3 G_N M_0}{R^3} e^{V_R - \psi}, \quad (3.29)$$

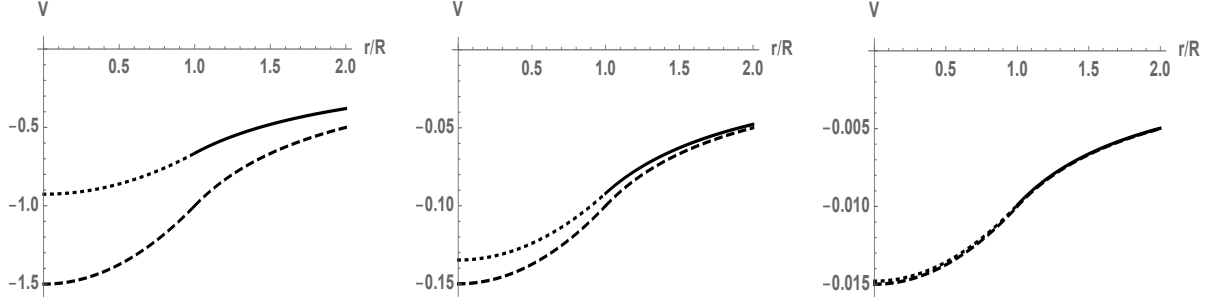


Figure 5: Potential  $V_{\text{out}}$  (solid line) *vs* approximate solution (3.24) (dotted line) *vs* Newtonian potential (dashed line), for  $G_N M/R = 1$  (left panel),  $G_N M/R = 1/10$  (center panel) and  $G_N M/R = 1/100$  (right panel).

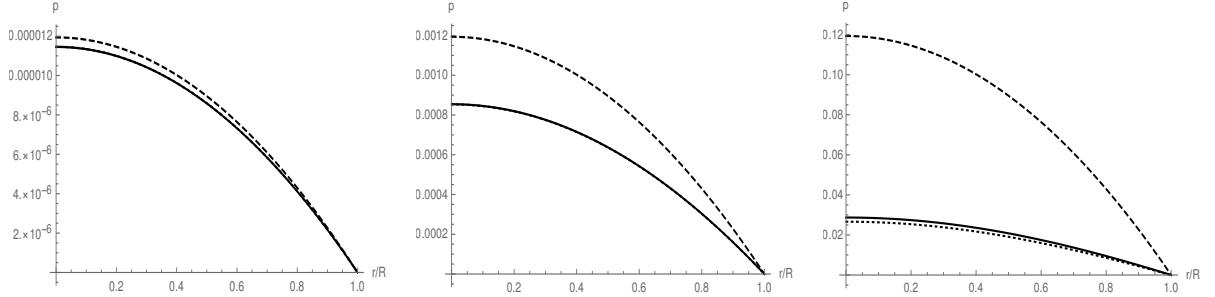


Figure 6: Pressure obtained from the expansion (3.18) (solid line) *vs* numerical pressure (dotted line) *vs* Newtonian pressure (3.28) (dashed line), for  $G_N M/R = 1/100$  (left panel),  $G_N M/R = 1/10$  (center panel) and  $G_N M/R = 1$  (right panel).

which is given by

$$\psi(r; A, B) = -A \left( B + \frac{r}{R} \right) + 2 \ln \left[ 1 + \frac{3 G_N M_0}{2 A^2 R} e^{A(B+r/R)+V_R} \right], \quad (3.30)$$

where the constants  $A$ ,  $B$  and  $M_0$  can be fixed (for any value of  $R$ ) by imposing the boundary conditions (3.3), (3.4) and (3.5). Regularity at  $r = 0$  in particular yields

$$M_0 = \frac{2 A^2 R}{3 G_N} e^{-A B - V_R}. \quad (3.31)$$

Eq. (3.5) for the continuity of the derivative across  $r = R$  then reads

$$A \tanh(A/2) = R V'_R. \quad (3.32)$$

For large compactness,  $R V'_R \sim (G_N M/R)^{2/3} \gg 1$ , and we can approximate the above equation as

$$A \simeq R V'_R. \quad (3.33)$$

The continuity Eq. (3.4) for the potential finally reads

$$2 \ln \left( 1 + e^{R V'_R} \right) - R V'_R (1 + B) = V_R, \quad (3.34)$$

and can be used to express  $B$  in terms of  $M$  and  $R$ . Putting everything together, we obtain

$$\begin{aligned}\psi(r; M, R) &\simeq \frac{1}{4} \left\{ 1 - \frac{1 + (2 G_N M/R) (1 + 2 r/R)}{(1 + 6 G_N M/R)^{1/3}} + 8 \ln \left[ \frac{1 + e^{\frac{G_N M r/R^2}{(1+6 G_N M/R)^{1/3}}}}{1 + e^{\frac{G_N M/R}{(1+6 G_N M/R)^{1/3}}}} \right] \right\} \\ &\simeq \frac{1}{2} \left( \frac{G_N M}{\sqrt{6} R} \right)^{2/3} \left( \frac{2r}{R} - 5 \right),\end{aligned}\quad (3.35)$$

and

$$\begin{aligned}\frac{M_0}{M} &\simeq \frac{G_N M/R}{3 (1 + 6 G_N M/R)^{2/3} \left\{ 1 + \cosh \left[ \frac{G_N M/R}{(1+6 G_N M/R)^{1/3}} \right] \right\}} \\ &\simeq \frac{1}{3} \left( \frac{2 G_N M}{9 R} \right)^{1/3} e^{-\left( \frac{G_N M}{\sqrt{6} R} \right)^{2/3}},\end{aligned}\quad (3.36)$$

in which we showed the leading behaviours for  $G_N M \gg R$ . It is important to remark that the condition (3.3) is not apparently satisfied by the above approximate expressions, although it was imposed from the very beginning, which shows once more how complex is to obtain analytical approximations for the problem at hand.

The solutions to the complete equation (3.15) could then be written as

$$V_{\text{in}} = f(r; A, B) \psi(r; A, B), \quad (3.37)$$

where  $A$ ,  $B$  and  $M_0$  should again be computed from the three boundary conditions, so that  $V_{\text{in}}$  eventually depends only on the parameters  $M$  and  $R$ . Since solving for  $f = f(r)$  is not any simpler than the original task, we shall instead just find lower and upper bounds, that is constants  $C_{\pm}$  such that

$$C_- < f(r) < C_+, \quad (3.38)$$

in the whole range  $0 \leq r \leq R$ . In particular, we consider the bounding functions

$$V_{\pm} = C_{\pm} \psi(r; A_{\pm}, B_{\pm}), \quad (3.39)$$

where  $A_{\pm}$ ,  $B_{\pm}$  and  $C_{\pm}$  are constants computed by imposing the boundary conditions (3.3), (3.4) and (3.5) and such that  $E_+(r) < 0$  and  $E_-(r) > 0$  for  $0 \leq r \leq R$ .

In details, we first determine a function  $V_C = C \psi(r; A, B)$  which satisfies the three boundary conditions for any constant  $C$ . Eq. (3.3) yields the same expression (3.31), whereas the l.h.s. of Eq. (3.32) is just rescaled by the factor  $C$  and continuity of the derivative therefore gives the approximate solution

$$C A \simeq R V_R'. \quad (3.40)$$

Eq. (3.4) for the continuity of the potential likewise reads

$$2 C \ln \left( 1 + e^{R V_R'/C} \right) - C R V_R' (1 + B) = V_R, \quad (3.41)$$

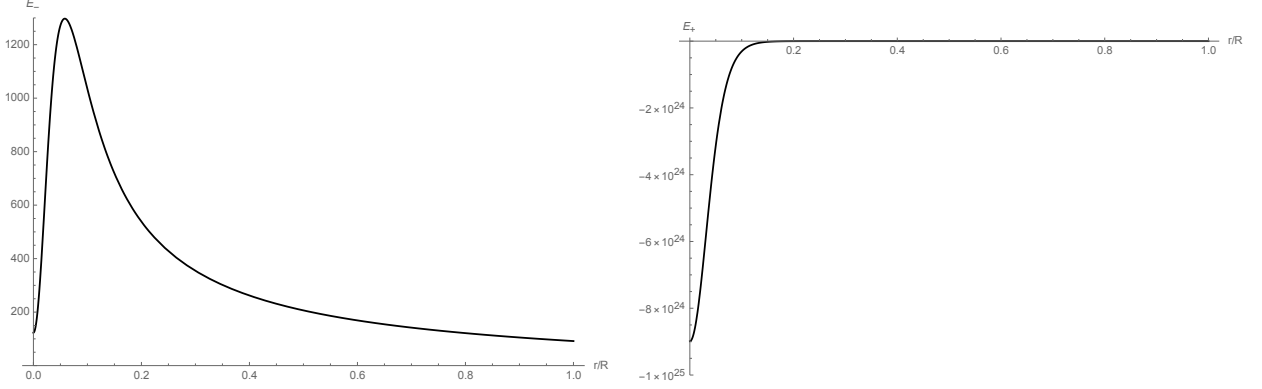


Figure 7: Left panel:  $E_-$  for  $C_- = 1$ . Right panel:  $E_+$  for  $C_+ = 1.6$ . Both plots are for  $G_N M/R = 10^3$ .

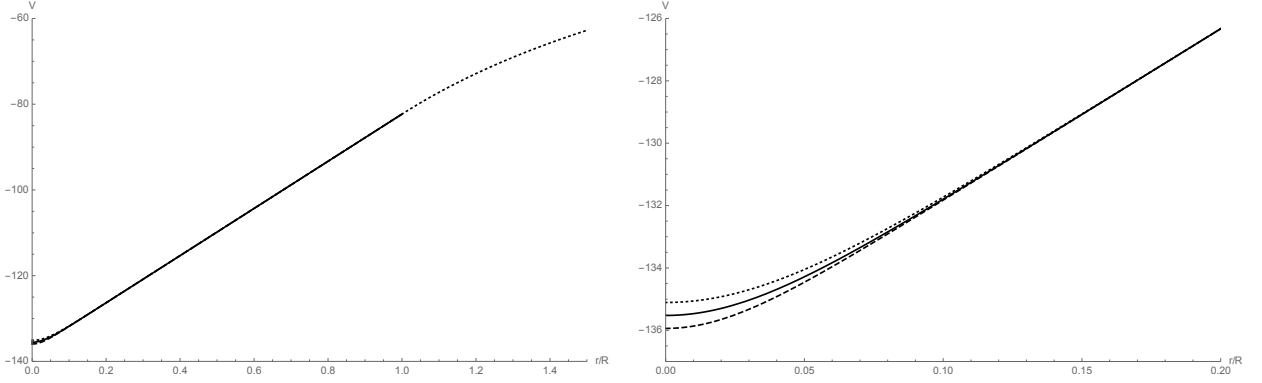


Figure 8: Left panel: approximate inner potentials  $V_-$  (dashed line),  $\tilde{V}$  (solid line) and  $V_+$  (dotted line) for  $0 \leq r \leq R$  and exact outer potential  $V_{\text{out}}$  (dotted line) for  $r > R$ . Right panel: approximate inner potentials  $V_-$  (dashed line),  $\tilde{V}$  (solid line) and  $V_+$  (dotted line) for  $0 \leq r \leq R/5$ . Both plots are for  $G_N M/R = 10^3$ .

Upon solving the above equations one then obtains  $V_C = C \psi(r; A(M, R, C), B(M, R, C))$  and  $M_0 = M_0(M, R, C)$ . For fixed values of  $R$  and  $M$ , one can then numerically determine a constant  $C_+$  such that  $E_+ < 0$  and a constant  $C_- < C_+$  such that  $E_- > 0$ .

For example, for the compactness  $G_N M/R = 10^3$ , we can use  $C_- \simeq 1$  and  $C_+ \simeq 1.6$ , and the plots of  $E_-$  and  $E_+$  are shown in Fig. 7. In particular, the minimum value of  $|E_+| \simeq 14$ . The corresponding potentials  $V_{\pm}$  along with  $\tilde{V} = \tilde{C} \psi$ , where  $\tilde{C} = (C_+ + C_-)/2$ , are displayed in Fig. 8. It is easy to see that the three approximate solutions essentially coincide almost everywhere, except near  $r = 0$  where they start to fan out, albeit still very slightly (the right panel of Fig. 8 shows a close-up of this effect). A similar behaviour is obtained for larger values of  $G_N M/R$ . For smaller values of the compactness up to  $G_N M/R \simeq 50$ , the approximation (3.40) is still quite accurate (see Fig. 9), even if the smaller the compactness the bigger the difference between  $V_{\pm}$ . Actually, the error in the derivative of the potential at  $r = R$  is of the order of 0.01% and 0.6% for  $G_N M/R = 10^2$  and  $G_N M/R = 50$ , respectively. In order to obtain a comparable precision for lower compactness, the approximate expression (3.40) should be improved, but we do not need to do that given how accurate is the perturbative expansion employed in Section 3.3.1.

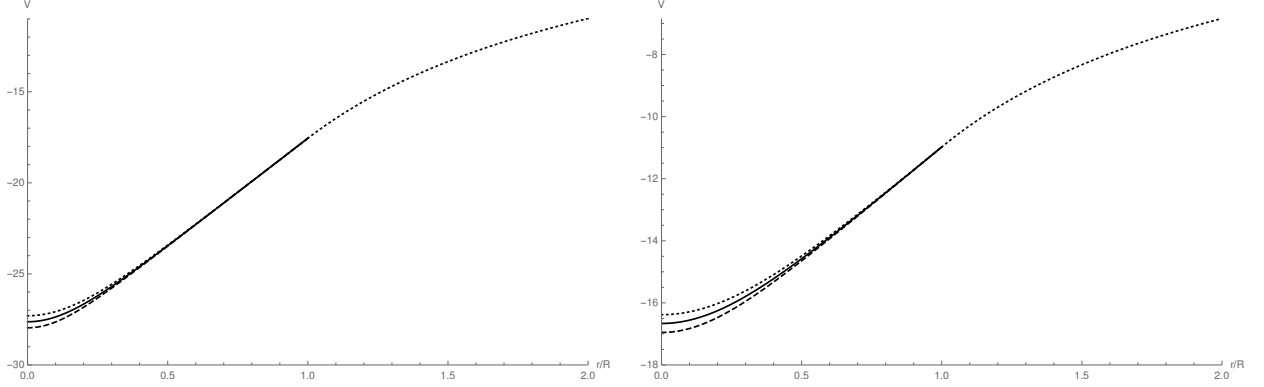


Figure 9: Approximate inner potentials  $V_-$  (dashed line),  $\tilde{V}$  (solid line) and  $V_+$  (dotted line) for  $0 \leq r \leq R$  and exact outer potential  $V_{\text{out}}$  (dotted line) for  $r > R$  and for  $G_N M/R = 10^2$  (left panel, with  $C_- = 1.042$  and  $C_+ = 1.52$ ) and  $G_N M/R = 50$  (right panel, with  $C_- = 1.073$  and  $C_+ = 1.5$ )

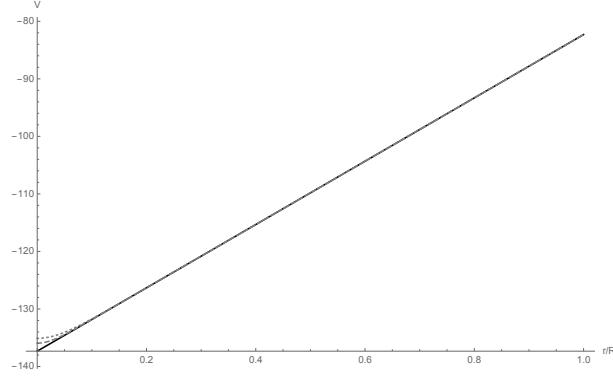


Figure 10: Approximate inner potentials  $V_-$  (dashed line),  $V_{\text{lin}}$  (solid line) and  $V_+$  (dotted line) for  $0 \leq r \leq R$ . Both plots are for  $G_N M/R = 10^3$ .

From the left panel of Fig. 8, it is clear that for  $G_N M/R = 10^3$  the potential  $V_{\text{in}}$  is practically linear, except near  $r = 0$  where it turns into a quadratic shape, in order to ensure the regularity condition (3.3). An approximate expression for the source proper mass  $M_0$  in terms of  $M$  can then be obtained from the simple linear approximation

$$V_{\text{lin}} \simeq V_R + V'_R (r - R) , \quad (3.42)$$

where  $V_R$  and  $V'_R$  are given by the usual expressions (3.9) and (3.10), and which is shown in Fig. 10 for  $G_N M/R = 10^3$ . Upon replacing the approximation (3.42) into the equation (3.15) for  $r = R$ , we obtain

$$\frac{M_0}{M} \simeq \frac{2(1 + 5 G_N M/R)}{3(1 + 6 G_N M/R)^{4/3}} . \quad (3.43)$$

The linear approximation is not very useful when it comes to evaluate the maximum value of the pressure, which we expect to occur in the origin at  $r = 0$ , precisely where this approximation must fail. We therefore consider again the approximation  $\tilde{V} = \tilde{C} \psi$ , which replaced into Eq. (3.14)

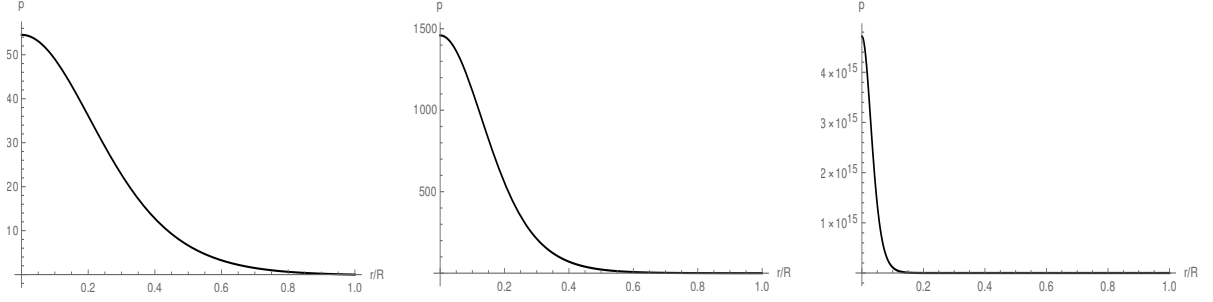


Figure 11: Pressure evaluated using the approximation  $\tilde{V} = \tilde{C}\psi$  for  $G_N M/R = 50$  (left panel),  $G_N M/R = 100$  (center panel) and  $G_N M/R = 1000$  (right panel). The constant  $\tilde{C} = (C_+ + C_-)/2$ , where  $C_+$  and  $C_-$  are the same as in Figs. 8 and 9 for the corresponding cases.

gives rise to the pressure shown in Fig. 11. Since the full expression is very cumbersome, we just show the leading order contribution for large compactness

$$p \simeq \frac{M^2 e^{\frac{1}{2} \left( \frac{G_N M}{\sqrt{6} R} \right)^{2/3} \left( 3 - \frac{5}{\tilde{C}} \right)}}{2 \pi \tilde{C}^2 (6 G_N M/R)^{2/3}} \left[ e^{\left( \frac{G_N M}{\sqrt{6} R} \right)^{2/3} \left( 1 - \frac{r}{R} \right)} - 1 \right], \quad (3.44)$$

which yields

$$p(0) \simeq \frac{M^2 e^{\frac{5}{2} \left( \frac{\tilde{C}-1}{\tilde{C}} \right) \left( \frac{G_N M}{\sqrt{6} R} \right)^{2/3}}}{2 \pi \tilde{C}^2 (6 G_N M/R)^{2/3}}, \quad (3.45)$$

where we find that  $\tilde{C} > 1$  for  $G_N M/R \gg 1$ . It is clear from this expression and Fig. 11 how rapidly the pressure grows near the origin when the compactness increases, but still remaining finite and regular everywhere even for very large compactness. In Fig. 12 we can see the comparison of the above approximate expression with the graphs shown in Fig. 11. Of course the bigger the compactness the more rapidly the approximation (3.44) approaches the results of Fig. 11. In Figs. 13 and 14 we instead plot the comparison between the approximation (3.44) with  $\tilde{C} = (C_+ + C_-)/2$  and the pressure evaluated from Eq. (3.14) and  $V_{\pm} = C_{\pm}\psi$ . The values of  $C_-$  and  $C_+$  are the same as in Figs. 8 and 9 for the corresponding compactness.

## 4 Horizon and gravitational energy

The approach we used so far completely neglects any geometrical aspect of gravity. In particular, it is well known that collapsing matter is responsible for the emergence of black hole geometries, providing us with the associated Schwarzschild radius (1.1). In general relativity, this marks the boundary between sources which we consider as stars ( $R \gg R_H$ ) and black holes ( $R \lesssim R_H$ ). Moreover, if the pressure is isotropic, stars must have a radius  $R > (9/8) R_H$ , known as the Buchdahl limit [10], otherwise the necessary pressure diverges.

We found that the pressure is always finite in our bootstrapped picture, hence there is no analogue of the Buchdahl limit. This means that the source can have arbitrarily large compactness, including  $R < R_H$ . Lacking precise geometrical quantities, we will follow a Newtonian argument

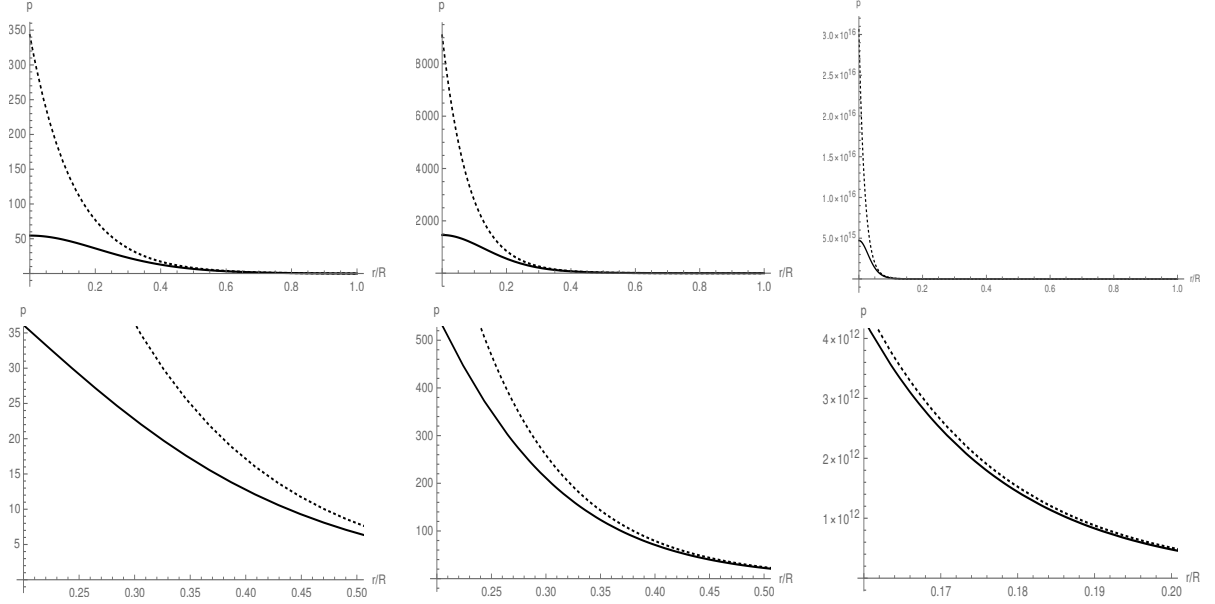


Figure 12: Comparison between the approximate pressure (11) (dotted line) *vs* solution of Eq. (3.44) with  $\tilde{V} = \tilde{C} \psi$  and  $\tilde{C} = (C_+ + C_-)/2$  (solid line) for  $G_N M/R = 50$  (top left panel),  $G_N M/R = 100$  (top central panel),  $G_N M/R = 1000$  (top right panel), and the corresponding close-ups in the bottom panels.

and define the horizon as the value  $r_H$  of the radius at which the escape velocity of test particles equals the speed of light, namely

$$2V(r_H) = -1, \quad (4.1)$$

as in Ref. [4]. Of course, when the source is diluted no horizon should exist and the above definition correctly reproduces this expectation, since that condition is never fulfilled for small compactness (see Figs. 2 and 3). In fact, we can find a limiting lower value for the compactness at which Eq. (4.1) has a solution, by requiring

$$2V_{\text{in}}(r_H = 0) = -1, \quad (4.2)$$

which gives  $G_N M/R \simeq 0.46$  if we use  $V(0) = V_0$  from Eq. (3.22). Upon increasing the compactness, the horizon radius  $r_H$  will increase and eventually approach the radius  $R$  of the matter source, which occurs when

$$2V_{\text{in}}(r_H = R) = 2V_{\text{out}}(R) = -1, \quad (4.3)$$

where  $V_{\text{out}}(R) = V_R$  is given by the exact expression in Eq. (3.9). This yields the compactness  $G_N M/R \simeq 0.69$  and  $r_H \simeq R \simeq 1.43 G_N M$ . For even larger values of the compactness, the horizon radius will always appear in the outer potential (3.7) and therefore remain fixed at this value in



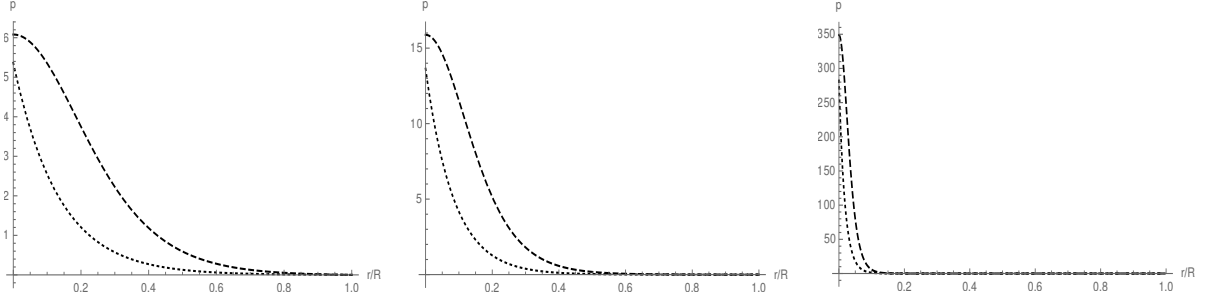


Figure 13: Pressure evaluated from  $V_- = C_- \psi$  (dashed line) *vs* pressure evaluated from  $\tilde{V} = \tilde{C} \psi$  (dotted line) for  $G_N M/R = 50$  (left panel),  $G_N M/R = 100$  (center panel) and  $G_N M/R = 1000$  (right panel).

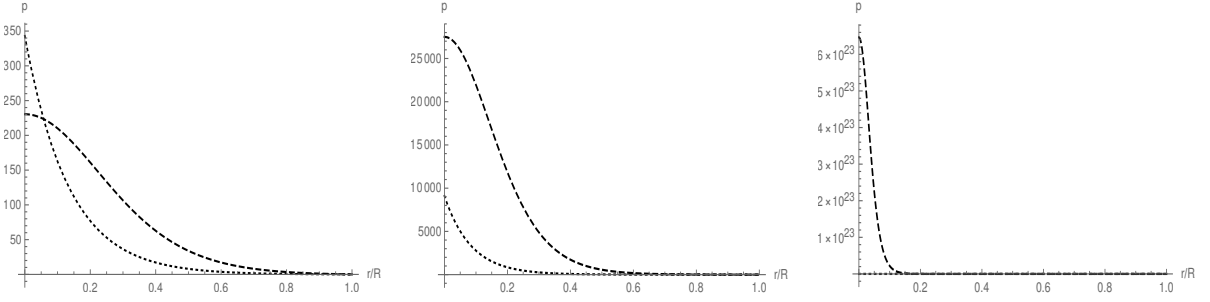


Figure 14: Pressure evaluated from  $V_+ = C_+ \psi$  (dashed line) *vs* pressure evaluated from  $\tilde{V} = \tilde{C} \psi$  with  $\tilde{C} = (C_+ + C_-)/2$  (dotted line) for  $G_N M/R = 50$  (left panel),  $G_N M/R = 100$  (center panel) and  $G_N M/R = 1000$  (right panel).

terms of  $M$ . We can summarise the situation as follows

$$\left\{ \begin{array}{ll} \text{no horizon} & \text{for } G_N M/R \lesssim 0.46 \\ 0 < r_H \leq R \simeq 1.4 G_N M & \text{for } 0.46 \lesssim G_N M/R \leq 0.69 \\ r_H \simeq 1.4 G_N M & \text{for } G_N M/R \gtrsim 0.69 . \end{array} \right. \quad (4.4)$$

The above values of the compactness further correspond to proper masses

$$\frac{M_0}{M} \simeq \left\{ \begin{array}{ll} 0.56 & \text{for } G_N M/R \simeq 0.46 \\ 0.47 & \text{for } G_N M/R \simeq 0.69 , \end{array} \right. \quad (4.5)$$

so that, when the horizon is precisely at the surface of the source, we have

$$r_H \simeq 1.4 G_N M \simeq 3 G_N M_0 . \quad (4.6)$$

It is also important to remark that the horizon  $r_H$  lies inside the source for a relatively narrow range of the compactness (see Fig. 15 for the corresponding potentials).

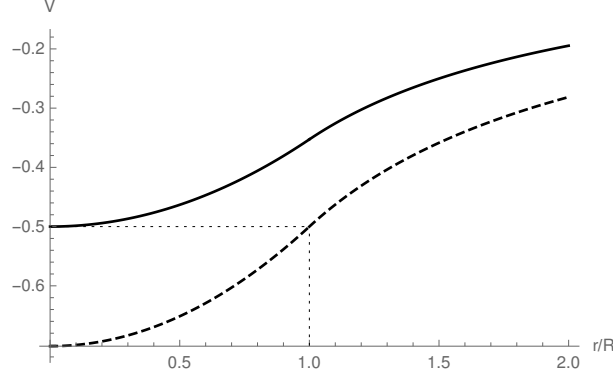


Figure 15: Potentials corresponding to  $r_H = 0$  (solid line) and  $r_H = R$  (dashed line).

We can next estimate the gravitational potential energy  $U_G$  from the effective Hamiltonian (2.8) (with  $q_\Phi = 1$ ). It is convenient to separate it into three different parts,

$$U_{BG} = 4\pi \int_0^\infty r^2 dr (\rho + p) V (1 - 2V) = \frac{3M_0}{R^3} \int_0^R r^2 dr e^{V_R - V_{in}} V_{in} (1 - 2V_{in}) \quad (4.7)$$

$$U_{GG}^{\text{in}} = \frac{1}{2G_N} \int_0^R r^2 dr (V'_{in})^2 (1 - 4V_{in}) \quad (4.8)$$

$$U_{GG}^{\text{out}} = \frac{1}{2G_N} \int_R^\infty r^2 dr (V'_{out})^2 (1 - 4V_{out}) , \quad (4.9)$$

where we simplified the first line with the help of Eq. (3.14). While the contribution from the outside is exactly given by

$$U_{GG}^{\text{out}} = \frac{G_N M^2}{2R} , \quad (4.10)$$

the inner contributions can only be evaluated within the approximations for the potential employed in the previous sections.

The energy contributions for objects of low compactness  $G_N M/R \ll 1$  can be evaluated straightforwardly. Starting from the approximate expression in (3.26) and (3.27) the total energy is calculated to be

$$U_G = U_{BG} + U_{GG}^{\text{in}} + U_{GG}^{\text{out}} \simeq -\frac{3G_N M^2}{5R} + \frac{9G_N^2 M^3}{7R^2} , \quad (4.11)$$

where we immediately notice the usual newtonian term at the lowest order.

One can also calculate the three components of the gravitational potential energy in the regime of intermediate compactness  $G_N M/R \sim 1$ , but the explicit expressions would be too cumbersome to display. Instead, the left panel of Fig. 16 shows a comparison in the regime of low compactness between the above expression for  $U_G$  and the one obtained starting from the analytic approximations from Eqs. (3.23) and (3.24), which are valid both for sources of low and intermediate compactness. It can be seen that the two approximations lead to similar results for objects that have low compactness. The center panel also shows the behaviour of  $U_G$  for objects of intermediate compactness. As expected, the gravitational potential energy becomes more and more negative as the density of the source increases.

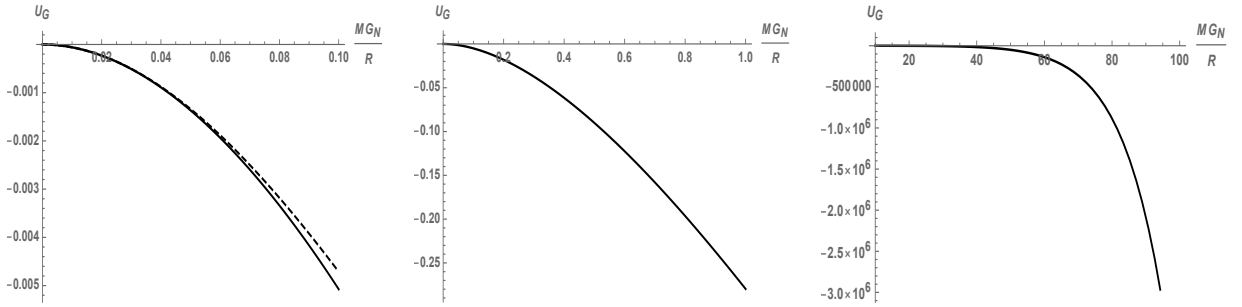


Figure 16: Total gravitational potential energy  $U_G$ . Left panel:  $U_G$  in the low compactness regime from the analytic approximations valid in the low and intermediate regime (continuous line) *vs*  $U_G$  from Eq. (4.11) (dashed line). Center panel:  $U_G$  in the low and intermediate compactness regime. Right panel:  $U_G$  in the high compactness regime.

We conclude with the high compactness regime, in which the increase in modulus of the negative gravitational potential energy is even more dramatic, as shown in the right panel of Fig. 16. To make things easier, we are going to evaluate the contributions (4.7) and (4.8) in the limit  $G_N M/R \gg 1$ , with the help of the linear approximation (3.42) and (3.43). The leading order in  $G_N M/R \gg 1$  then reads

$$U_{BG} \simeq -\frac{125 R}{3 G_N} e^{\left(\frac{G_N M}{\sqrt{6} R}\right)^{2/3}} \quad (4.12)$$

and

$$U_{GG}^{\text{in}} \simeq \frac{5 G_N M^2}{36 R} . \quad (4.13)$$

One expects that this negative and large potential energy  $U_G$  is counterbalanced by the positive energy (C.11) associated with the pressure (3.44) inside the matter source.

Of course, the total energy of the system should still be given by the ADM-like mass  $M$ , which must therefore equal the sum of the matter proper mass  $M_0$  and the energy associated with the pressure (see Appendix C for more details about the energy balance).

## 5 Conclusions and (quantum) outlook

In this work we have fully developed a bootstrapped model of isotropic and homogeneous stars, in which the pressure and density both contribute to the potential describing the gravitational pull on test particles. No equivalent of the Buchdahl limit was found, and the matter source can therefore be kept in equilibrium by a sufficiently large (and finite) pressure for any (finite) value of the compactness  $G_N M/R$ . When the compactness of the source exceeds a value of order 0.46, a horizon appears inside the source and its radius  $r_H \simeq R$  for  $G_N M/R \simeq 0.69$ . For larger values of the compactness, the source is entirely inside  $r_H$  and we can consider cases with  $r_H \gtrsim R$  as representing bootstrapped Newtonian black holes.

When the matter is collapsed further inside the horizon, that is for larger compactness such that  $r_H \gg R$ , the gravitational potential energy grows even more negative, and a correspondingly very

large pressure  $p$  is required in order to support the matter core. In fact, if we assume that black holes have regular inner cores of finite proper mass  $M_0$  and thickness  $R$ , from Eq. (3.43) we obtain

$$\frac{G_N M_0}{R} \sim \left( \frac{G_N M}{R} \right)^{2/3}, \quad (5.1)$$

so that  $M_0/M \sim (R/G_N M)^{1/3}$  for  $G_N M/R \gg 1$ . This means that most of the matter energy must be accounted for by the interactions that give rise to the pressure in very compact sources. Such a huge pressure  $p \gg \rho$  could only be of purely quantum nature, thus requiring a quantum description of the matter in the source.

Correspondingly, the regular potential we obtained in the present work should be viewed as the mean field description of the quantum state of the (off-shell) gravitons in a (regular <sup>3</sup>) black hole when  $R \lesssim r_H$ . It will be therefore a natural development to investigate the quantum features of this potential, as it affects both the quantum state of matter inside the black hole (or falling into it) and the dynamics of the gravitons themselves. Eventually, one would also like to identify the fully quantum state that generates this potential, like it was done for the Newtonian potential in Refs. [6, 18], or in Refs. [23, 24]. Finally, we would like to remark that, although we found that  $M \gg M_0$  for very large compactness, and one could thus infer that matter become almost irrelevant inside a black hole [15], the above picture inherently requires the presence of matter, whose role in black hole physics we believe needs more investigations [19–22].

## Acknowledgments

R.C. and M.L. are partially supported by the INFN grant FLAG. The work of R.C. has also been carried out in the framework of activities of the National Group of Mathematical Physics (GNFM, INdAM) and COST action *Cantata*. O.M. is supported by the grant Laplas VI of the Romanian National Authority for Scientific Research.

## A Newtonian solution

We recall that the Newtonian solution of the Poisson equation (2.2) with a homogeneous source of mass  $M_0$  and radius  $R$ ,

$$\Delta V_N = \frac{3 G_N M_0}{R^3} \Theta(R - r), \quad (A.1)$$

is given by

$$V_N = \begin{cases} \frac{G_N M_0}{2 R^3} (r^2 - 3 R^2) & \text{for } 0 \leq r < R \\ -\frac{G_N M_0}{r} & \text{for } r > R, \end{cases} \quad (A.2)$$

which is continuous, with continuous first derivative across  $r = R$ . We also remark that there is one and the same mass parameter  $M_0 = M$  in the interior and exterior part of the potential.

---

<sup>3</sup>For a review, see Ref. [25]

## B Comparison method

We have shown in Section 3.3 that a solution to Eq. (3.15) satisfying Eq. (3.17) exists by employing comparison functions [12, 13] and we recall the fundamentals of this method here for the sake of convenience.

Let us consider an equation of the form

$$u''(r) = F(r, u(r), u'(r)) , \quad (\text{B.1})$$

where  $F$  is a real function of its arguments,  $r$  varies in the finite interval  $[r_1, r_2]$  and a prime denotes the derivative with respect to  $r$ . We want to find a solution which further satisfies the general boundary conditions

$$a_1 u(r_1) - a_2 u'(r_1) = A_0 , \quad (\text{B.2})$$

$$b_1 u(r_2) + b_2 u'(r_2) = B_0 , \quad (\text{B.3})$$

with  $A_0, B_0, a_1, b_1$  real numbers and  $a_2, b_2$  non negative real numbers satisfying  $a_1^2 + a_2^2 > 0$  and  $b_1^2 + b_2^2 > 0$ . The theorems in Refs. [12, 13] guarantee that such a solution  $u \in C^2([r_1, r_2])$  exists under the following three conditions:

1. we can find a lower bounding function

$$u''_-(r) \geq F(r, u_-(r), u'_-(r)) \quad (\text{B.4})$$

$$a_1 u_-(r_1) - a_2 u'_-(r_1) \leq A_0 \quad (\text{B.5})$$

$$b_1 u_-(r_2) + b_2 u'_-(r_2) \leq B_0 , \quad (\text{B.6})$$

and an upper bounding function

$$u''_+(r) \leq F(r, u_+(r), u'_+(r)) \quad (\text{B.7})$$

$$a_1 u_+(r_1) - a_2 u'_+(r_1) \geq A_0 \quad (\text{B.8})$$

$$b_1 u_+(r_2) + b_2 u'_+(r_2) \geq B_0 ; \quad (\text{B.9})$$

2. the function  $F$  is continuous on the domain  $D = \{(r, u, u') \in [r_1, r_2] \times \mathbb{R}^2 \mid u_- \leq u \leq u_+\}$ ;
3. the function  $F$  satisfies a *Nagumo condition*: there exists a continuous and positive function  $\phi$  such that

$$\int_0^\infty \frac{s \, ds}{\phi(s)} = \infty \quad (\text{B.10})$$

and,  $\forall (t, u, u') \in D$ ,

$$|F(r, u(r), u'(r))| \leq \phi(|u'|) . \quad (\text{B.11})$$

Moreover, the solution  $u$  will satisfy

$$u_-(t) \leq u(t) \leq u_+(t) . \quad (\text{B.12})$$

We can now apply the above general theorem to our problem inside the source, for which  $r_1 = 0$  and  $r_2 = R$ . We first rewrite Eq. (3.15) as

$$\begin{aligned} V'' &= \frac{3 G_N M_0}{R^3} e^{V_R - V} + \frac{2 (V')^2}{1 - 4V} - \frac{2 V'}{r} \\ &\equiv F(r, V, V') , \end{aligned} \quad (\text{B.13})$$

and recall the boundary conditions (3.3) and (3.4), that is

$$V'(0) = 0 \quad (\text{B.14})$$

$$V(R) = V_R . \quad (\text{B.15})$$

We can now verify all the requirements of the theorem, and will do so for the case of large compactness analysed in Section 3.3.2. The upper and lower bounding functions are therefore  $V_{\pm}$  given in Eq. (3.39) and the domain

$$D = \{(r, V, V') \in [0, R] \times \mathbb{R}^2 \mid V_- \leq V \leq V_+ \} . \quad (\text{B.16})$$

Continuity of  $F$  on  $D$  is easily verified. In fact, the first term on the right hand side of Eq. (B.13) is an exponential of  $V$  which is always regular in  $D$ . The same is true for the second term considering that  $V_{\pm} < 0$ , thus  $V < 0$  as well. The last term could be tricky but the boundary condition (B.14) require that  $V'$  vanishes at  $r = 0$  at least as fast as  $r$  [see the expansion around  $r = 0$  in Eq. (3.18)] so that this is also regular in  $D$ . Finally, we can choose

$$\phi = \max_D(F) , \quad (\text{B.17})$$

which must be finite given that  $F$  is continuous in  $D$ .

All of the hypotheses of the theorem hold and a solution to Eq. (3.15) therefore exists and satisfies Eq. (3.17). By imposing the remaining boundary condition (3.5), one can then obtain a relation between  $M_0$ , which appears in the equation (3.15), and  $M$ , which appears in the boundary conditions (3.4) and (3.5), for any given value of  $R$ .

## C Energy balance

In Section 4, we only computed the gravitational energy from the Hamiltonian (2.8). The purely baryonic contribution will be given by the proper mass  $M_0$  and the pressure energy contribution found again from the newtonian argument (2.6), whereby

$$U_B(R) = D(M, R) - 4\pi \int_0^R r^2 dr p(r) . \quad (\text{C.1})$$

In the newtonian regime, the integration constant  $D(M, R)$  can be fixed so as to guarantee that the work done by gravity is equal and opposite to the work done by the forces responsible for the pressure  $p$ . In other words, in that case we find  $D(M, R)$  by requiring that the gravitational force is conservative. This will also ensure that the total energy related to the Hamiltonian constraint equals the ADM-like mass  $M$  of the system, that is

$$E = M_0 + U_G + U_B = M . \quad (\text{C.2})$$

Of course, in the Newtonian case Eq. (C.2) simply reads  $E = M_0 \equiv M$ , as shown in Ref. [4].

In the bootstrapped picture, gravity is not a linear interaction any more and it is not at all obvious that it will still be conservative. A precise energy estimate would therefore require a complete knowledge of the dynamical process which led to the formation of the equilibrium configuration of given ADM-like mass  $M$  and radius  $R$ . Without that knowledge, we can only assume that the total energy of the equilibrium configuration equals  $M$  and fix  $D(M, R)$  so that the Hamiltonian constraint (C.2) is satisfied.

With that prescription, we can now evaluate the baryonic contributions. In the low compactness case, we expand all the terms in Eq. (C.2) to order  $M^3$ , namely

$$M_0 \simeq M - \frac{5 G_N M^2}{2 R} + \frac{81 G_N^2 M^3}{8 R^2} , \quad (\text{C.3})$$

and the pressure energy

$$U_B \simeq D_s(M, R) - \frac{G_N M^2}{5 R} + \frac{61 G_N^2 M^3}{70 R^2} . \quad (\text{C.4})$$

Eq. (C.2) is then satisfied for

$$D_s(M, R) \simeq -\frac{33 G_N M^2}{10 R} + \frac{3439 G_N^2 M^3}{280 R^2} \quad (\text{C.5})$$

so that

$$U_B \simeq \frac{31 G_N M^2}{10 R} \left( 1 - \frac{6390 G_N M}{1736 R} \right) , \quad (\text{C.6})$$

which is positive only for small compactness, as its approximation requires.

The high compactness regime of course yields quite different results. To make things easier, we again look at the limiting case of very high compactness, where the linear approximation (3.42) holds, and consider the Hamiltonian constraint (C.2) only at leading order in  $M$ . The proper mass in Eq. (3.43) can be simplified further to give

$$M_0 \simeq \frac{5 M}{9 (6 G_N M/R)^{1/3}} , \quad (\text{C.7})$$

while the pressure energy can be written as

$$U_B \simeq D_b(M, R) - \frac{20 R^3}{G_N^3 M^2} \left( \frac{G_N M}{\sqrt{6} R} \right)^{2/3} e^{\left( \frac{G_N M}{\sqrt{6} R} \right)^{2/3}} . \quad (\text{C.8})$$

Again, we just impose Eq. (C.2) and find

$$D_b(M, R) \simeq M + \frac{20 R^3}{G_N^3 M^2} \left( \frac{G_N M}{\sqrt{6} R} \right)^{2/3} e^{\left( \frac{G_N M}{\sqrt{6} R} \right)^{2/3}} + \frac{125 R}{3 G_N} e^{\left( \frac{G_N M}{\sqrt{6} R} \right)^{2/3}} \quad (\text{C.9})$$

$$-\frac{7 G_N M^2}{36 R} - \frac{5 M}{9 (6 G_N M/R)^{1/3}} , \quad (\text{C.10})$$

so that

$$U_B \simeq \frac{125 R}{3 G_N} e^{\left( \frac{G_N M}{\sqrt{6} R} \right)^{2/3}} , \quad (\text{C.11})$$

which is positive as it should, and precisely counterbalances Eq. (4.12).

## References

- [1] S. W. Hawking and G. F. R. Ellis, “The Large Scale Structure of Space-Time,” (Cambridge University Press, Cambridge, 1973)
- [2] R. P. Geroch and J. H. Traschen, Phys. Rev. D **36** (1987) 1017 [Conf. Proc. C **861214** (1986) 138]; H. Balasin and H. Nachbagauer, Class. Quant. Grav. **10** (1993) 2271 [gr-qc/9305009].
- [3] R. Brustein and A. J. M. Medved, “Non-singular black holes interiors need physics beyond the standard model,” arXiv:1902.07990 [hep-th]; Phys. Rev. D **99** (2019) 064019 [arXiv:1805.11667 [hep-th]].
- [4] R. Casadio, M. Lenzi and O. Micu, Phys. Rev. D **98** (2018) 104016 [arXiv:1806.07639 [gr-qc]].
- [5] R. Casadio, A. Giugno and A. Giusti, Phys. Lett. B **763** (2016) 337 [arXiv:1606.04744 [gr-qc]].
- [6] R. Casadio, A. Giugno, A. Giusti and M. Lenzi, Phys. Rev. D **96** 044010 (2017) [arXiv:1702.05918 [gr-qc]].
- [7] G. Schäfer and P. Jaranowski, Living Rev. Rel. **21** (2018) 7 [arXiv:1805.07240 [gr-qc]].
- [8] R.L. Arnowitt, S. Deser and C.W. Misner, Phys. Rev. **116** (1959) 1322.
- [9] R. Carballo-Rubio, F. Di Filippo and N. Moynihan, “Taming higher-derivative interactions and bootstrapping gravity with soft theorems,” arXiv:1811.08192 [hep-th]; S. Deser, Gen. Rel. Grav. **1** (1970) 9 [gr-qc/0411023]; Gen. Rel. Grav. **42** (2010) 641 [arXiv:0910.2975 [gr-qc]].
- [10] H. A. Buchdahl, Phys. Rev. **116** (1959) 1027.
- [11] N. Dadhich, Curr. Sci. **109** (2015) 260 [arXiv:1206.0635 [gr-qc]].
- [12] C. De Coster and P. Habets, “Two-Point Boundary Value Problems: Lower and Upper Solutions,” (Elsevier, Oxford, 2006).
- [13] R. Gaines, J. Differential Equations **12** (1972) 291; K. Schmitt, J. Differential Equations **7** (1970) 527.
- [14] A.C. King, J. Billingham, and S.R. Otto, “Differential equations: linear, nonlinear, ordinary, partial,” (Cambridge University Press, Cambridge, 2003)
- [15] G. Dvali and C. Gomez, JCAP **01** (2014) 023; “Black Hole’s Information Group”, arXiv:1307.7630; Eur. Phys. J. C **74** (2014) 2752 [arXiv:1207.4059 [hep-th]]; Phys. Lett. B **719** (2013) 419 [arXiv:1203.6575 [hep-th]]; Phys. Lett. B **716** (2012) 240 [arXiv:1203.3372 [hep-th]]; Fortsch. Phys. **61** (2013) 742; G. Dvali, C. Gomez and S. Mukhanov, “Black Hole Masses are Quantized,” arXiv:1106.5894 [hep-ph].
- [16] A. Giusti, Int. J. Geom. Meth. Mod. Phys. **16** (2019) no.03, 1930001.
- [17] R. Casadio, A. Giugno and A. Orlandi, Phys. Rev. D **91** (2015) 124069 [arXiv:1504.05356 [gr-qc]].
- [18] W. Mück, Eur. Phys. J. C **73** (2013) 2679 [arXiv:1310.6909 [hep-th]]; W. Mück and G. Pozzo, JHEP **1405** (2014) 128 [arXiv:1403.1422 [hep-th]].



- [19] V. F. Foit and N. Wintergerst, Phys. Rev. D **92** (2015) 064043 [arXiv:1504.04384 [hep-th]].
- [20] F. Kühnel, Phys. Rev. D **90** (2014) 084024 [arXiv:1312.2977 [gr-qc]]; F. Kühnel and B. Sundborg, JHEP **1412** (2014) 016 [arXiv:1406.4147 [hep-th]];
- [21] F. Kühnel and M. Sandstad, Phys. Rev. D **92** (2015) 124028 [arXiv:1506.08823 [gr-qc]].
- [22] G. Dvali and A. Gußmann, Nucl. Phys. B **913** (2016) 1001 [arXiv:1605.00543 [hep-th]].
- [23] R. Casadio, A. Giugno, O. Micu and A. Orlandi, Phys. Rev. D **90** (2014) 084040 [arXiv:1405.4192 [hep-th]].
- [24] R. Casadio and A. Orlandi, JHEP **1308** (2013) 025 [arXiv:1302.7138 [hep-th]]; R. Casadio, A. Giugno, A. Giusti and O. Micu, Eur. Phys. J. C **77** (2017) 322 [arXiv:1701.05778 [gr-qc]].
- [25] P. Nicolini, Int. J. Mod. Phys. A **24** (2009) 1229 [arXiv:0807.1939 [hep-th]].